Interim Report 2018

Development and Improvement of Flow Models Applied to Multiphase Flows in Large-Diameter Pipes and High-Velocity Flows

US Department of the Interior
Bureau of Ocean Energy Management
Gulf of Mexico OCS Region

Development and Improvement of Flow Models Applied to Multiphase Flows in Large-Diameter Pipes and High-Velocity Flows

Authors:

Francisco Bruno Xavier Teles
Paulo J. Waltrich
Matheus Sigaki Capovilla
Ipsita Gupta
Richard Hughes

Craft & Hawkins Department of Petroleum Engineering
Louisiana State University, Baton Rouge

US Department of the Interior
Bureau of Ocean Energy Management
Gulf of Mexico OCS Region

BOEM
Bureau of Ocean Energy Management

TABLE OF **C**ONTENTS

LIST OF FIGURES

LIST OF TABLES

ABBREVIATIONS AND ACRONYMS

BOEM	Bureau of Ocean Energy Management
WCD	Worst Case Discharge
IPR	Inflow Performance Relationship
TPR	Tubing Performance Relationship
BHP	Bottomhole Pressure [psi]
GLR	Gas Liquid Ratio [SCF/STB]
q_L	Liquid Ratio [BBL/d]
ID	Pipe Inner Diameter [in]
ρ	Density [lb/ft^3]
g	Gravitational Acceleration [32.2 ft/s^2]
d^*	Dimensionless Diameter
V_{sg}	Gas Superficial Velocity [ft/s]
V_{sg}	Liquid Superficial Velocity [ft/s]

1. ABSTRACT

This work proposes a model developed at LSU (called here as Teles and Waltrich model) that can determine pressure gradient in all flow regimes considering the concept of small and large diameter pipes. A series of field and experimental dataset for air-water, oil-natural gas systems are tested for a wide range of conditions in order to validate this model. The main objective of this study is to evaluate the performance of Teles and Waltrich model and other models commonly used in worst-case-discharge (WCD) calculations.

The scenarios for WCD calculations in most of the offshore drilling operations occurs in situations with high oil and gas flow rates, large diameters and high pressure flows. An important part of WCD calculations is the determination of the pressure variation during the multiphase flow of oil, gas, sand and water in the wellbore during a blowout, which involves the use of multiphase flow correlations. These correlations are developed from different empirical and mechanistic multiphase flow models, being most of them flow regime dependent. However, most of these models were originally developed and validated for air-water two-phase flows, for low pressures, and for pipe diameters much smaller than the ones usually encountered in the offshore wells. There is an understanding that the fluid behavior changes considerably from small to large diameters, mainly regarding the observation of churn flow regime for large-diameter pipes, when slug flow would be expected in small diameters. In addition, most of these models available in commercial packages (often used for WCD calculations) do not consider the presence of churn flow regime, and the use of slug flow models may leads to significant errors.

The comparison between model results and experimental and field data indicates that the use of slug flow model can lead to errors substantially higher than churn flow models. These results suggest that the use of Teles and Waltrich model, which includes a churn flow model, should be used for WCD calculations to obtain more accurate results. Some of the analysis also show that, at high pressures, _slug flow might not be present for oil-gas flows for diameters as small as 1 inch!_ The application of flow regime models for slug flow for pipe diameters between 1 and 4 inches is widely used in empirical and mechanistic models in the oil and gas industry. This may deliver erroneous results, as wellbore flow models will try to predict churn flow regime using a slug flow model. For this reason, it is crucial to implement the concept of small and large diameter presented in this report in wellbore flow models for a reliable prediction of pressure gradient in vertical two-phase flow in pipes.

2. INTRODUCTION

Vertical gas-liquid two-phase upward flow can be found in a wide range of industrial applications such as in offshore risers in the petroleum industry, cooling towers in the nuclear industry, and in gas-liquid pipelines in petrochemical plants. A typical example of a problem that requires the knowledge about vertical two-phase upward flow in pipes is in worst-case-discharge (WCD) calculations. The Bureau of Ocean Energy Management (BOEM) defined the WCD rate as the maximum uncontrollable daily flow rate of hydrocarbons through an unobstructed wellbore (SPE, 2015). In other words, WCD rate is the maximum expected flow rate during a blowout, considering the absence of an in-hole drillstring and a wellhead.

Recent new regulations requires from any operator company a report describing the plans to drill new wells in the Gulf of Mexico the submission of an Oil Spill Response Plan (OSRP), which should include a contingency plan to be followed in case of a blowout (Buchholz et al., 2016). An estimative of WCD rate is required in this type of report. Two main characteristics of the flow in the wellbore are expected during WCD events: high flow rates in large-diameter long-vertical pipes. OSRP reports present WCD flow rates in the Gulf of Mexico ranging from 0.63 to 75,678 m^3/day (4 to 476,000 bbl/day), averaging for the Central Gulf of Mexico about 9,540 m^3/day (60,000 bbl/day), and for the Western Gulf of Mexico about 2,225 m^3/day (14,000 bbl/day) (Buchholz et al., 2016). Furthermore, Zulqarnain (2015) described a representative well configuration based on statistical analysis about the current wells in the Gulf of Mexico, in which the average pipe diameter is about 0.25 m (~10 in).

Some studies have been carried out on multiphase flow in pipes of large diameter (Hernandez-Perez, Zangana, Kaji, & Azzopardi, 2010; A. Ohnuki & Akimoto, 1996; Akira Ohnuki & Akimoto, 2000; Omebere-Iyari, Azzopardi, & Ladam, 2007; Schoppa, Zabaras, Menon, & Wicks, 2013). However, there is still a lack of investigation about flows in larger diameter pipes and high flow rates.

Most mathematical models developed for vertical two-phase flow in pipes are based on experimental and field data for small diameter pipes (e.g., ID < 0.10 m - or ~4 in) and low liquid velocities, typically lower than 1 m/s (Omebere- Iyari et al., 2007; Smith, Schlegel, Hibiki, & Ishii, 2012). Thus, the applicability of such models to conditions involving large diameter and high-velocity flows is still questionable. Therefore, it is evident that studies are still needed on evaluating wellbore flow models and proposing improvements for its application on WCD calculations.

2.1 WORST CASE DISCHARGE RATE CALCULATION

In 2015, SPE released a technical report addressing the calculation of WCD rates (SPE, 2015). This calculation is based on a technique used for prediction of production rates as a function of the reservoir characteristics and the pressure drop along the flowing wellbore. This method is called nodal analysis (see Figure 1.b). It makes use of the inflow and outflow performance curves to calculate the flow rate of a well. The inflow performance relationship (IPR) represents the fluid flow in the reservoir (fluid flow through a porous medium) and the outflow performance relationship, also known as tubing performance relationship (TPR), represents the wellbore (fluid flow in pipes). Petroleum production systems, as shown in Figure 1.a, often deal with a relatively narrow range of wellbore pipe effective diameters, from 0.04 to 0.15 m (~1.5 to ~6 in), and flow rates lower than 1,600 m3/day (~10,000 bbl/day) (Takacs, 2001). On the other hand, WCD conditions involve higher two-phase fluid flow rates (possibly higher than 16,000 m^3/day, or ~100,000 bbl/day) and mostly larger pipe diameters (up to 0.50 m or ~20 in). Some recent studies (Ali, 2009; Omebere-Iyari et al., 2007; Schoppa et al., 2013) reported relevant differences concerning the multiphase flow dynamics in large-diameter vertical pipes when compared to small-diameter pipes. When not considered, these differences in pipe diameters can be translated into erroneous predictions of pressure drops for the wellbore and, consequently, inaccurate WCD rate calculations.

Waltrich et al. (2017) tested several different models used in WCD calculations against experimental pressure gradient data of upward two-phase flow in large diameter pipes. Most models showed errors larger than 50% for the pressure gradient predictions. Thus, tracking the elements that lead these models to large levels of uncertainty is necessary.

| (a) | (b) |
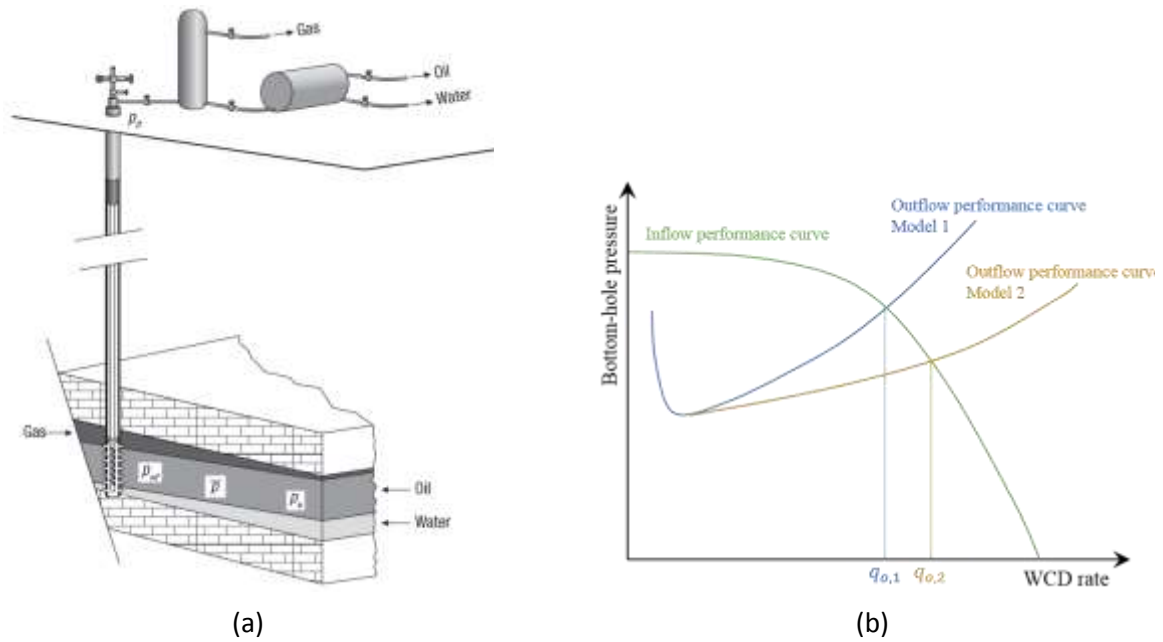
Figure 1 – Elements required for the prediction of production rates, being (a) a schematic of a petroleum production system, including the reservoir, completion, well, wellhead assembly, and surface facilities extracted from Economides, Hill, Ehlig-Economides, and Zhu (2012), and (b) an example of a nodal analysis plot, including an inflow performance curve and two outflow performance curves, each one calculated using different models.

2.2 TWO PHASE FLOW REGIMES IN VERTICAL PIPES

Figure 2 presents a simplified diagram for the calculation of WCD rates. As it can be seen, regarding the outflow performance curve, the determination of flow regimes has a direct impact in WCD calculations.

Flow regime prediction is a crucial part of two-phase flow analysis, since many multiphase flow models are flow regime dependent. Two-phase flow regimes are described by Shoham (2006) as a group of similar geometrical distribution of the gas and liquid phases in a pipe during a two-phase flow. Although it is possible to find several different vertical upward two-phase flow regimes characterizations throughout the literature, the four flow regimes listed below are most commonly defined in upward gas-liquid two-phase flow in vertical pipes. Figure 3 illustrates Bubbly, Slug, Churn, and Annular flow regimes.
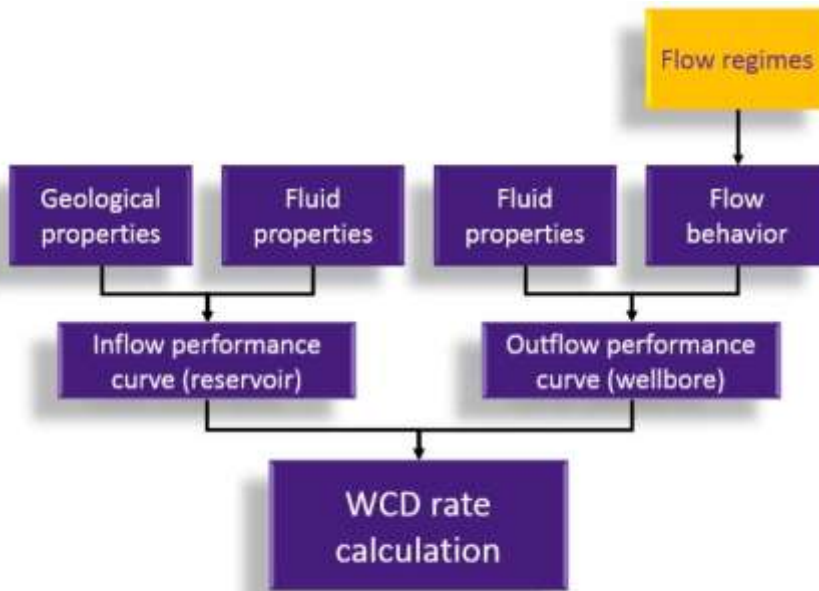
Figure 2 – Simplified diagram for WCD rate calculation.
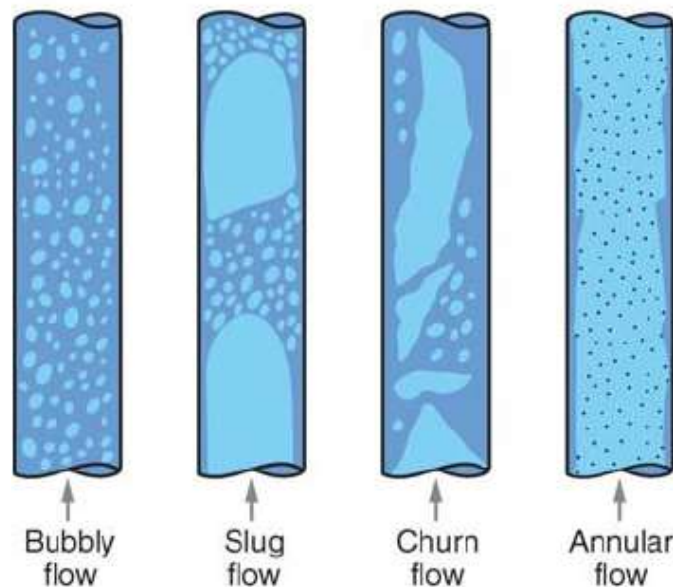
Figure 3 – Visual representation of the four main flow regimes during upward flow in vertical pipe, namely: bubbly flow, slug flow, churn flow, and annular flow. Source: Guet and Ooms (2005).

- Bubbly flow: This regime occurs when there are relatively low gas velocities and high liquid velocities. The continuous liquid phase flows carrying dispersed gas bubbles. Both phases move upward.
- Slug flow: This flow is characterized when there are a higher gas velocity and the bubbles get closer and coalesce forming a series of slug units. These slug units are composed by bullet shaped bubbles (also called Taylor bubbles) containing small bubbles dispersed within them. They are axially symmetrical and occupy almost the diameter of the pipe. There is a thin liquid film moving downward between the Taylor bubbles and the pipe wall as the gas flows upwards.

8

- Churn flow: For even higher gas velocities, these large bubbles are not stable anymore, and there is a chaotic movement of both gas and liquid phases in the downward and upward directions. There is no clear boundary between the phases.
- Annular flow: This occurs for very high gas velocities and it is characterized by a continuous fast-moving gas core with some liquid-phase droplets entrained, while the liquid-phase forms a continuous thin layer on the pipe wall flowing upwards.

2.3 CLASSIFICATION OF SMALL AND LARGE PIPE DIAMETERS

The flow regime determination is assumed by many investigators as the central problem in the field of multiphase flow in pipes (Shoham, 2006). Recent studies have pointed out the significant difference of flow regime behavior in small and large diameter pipes (Ali Shazia & Yeung, 2013; Akira Ohnuki & Akimoto, 2000; Wu et al., 2017). Among these differences, the absence of slug flow in large pipe diameters has been evident in several studies (Ali Shazia & Yeung, 2013; Capovilla, Cavalcanti de Sousa, & Waltrich, 2017; Cheng, Hills, & Azzorpardi, 1998; Hibiki & Ishii, 2000; Kataoka & Ishii, 1987; Akira Ohnuki & Akimoto, 2000; Omebere-Iyari et al., 2007; Shoukri, Hassan, & Gerges, 2008; Wu et al., 2017), thus, it should be considered in two phase flow models.

The work of Schlegel et al. (2009) discusses that small and large diameter pipes should be differentiated using the dimensionless diameter criterion defined by Kataoka and Ishii (1987), which is represented by equation 2.1. This dimensionless diameter determination considers the surface tension and gas-liquid densities, and it can be used to estimate the maximum diameter size for slug flow to occur in a vertical two-phase flow,

$$d^* = d \sqrt{\frac{g(\rho_l - \rho_g)}{\sigma}} \tag{2.1}$$

where σ is the surface tension between gas and liquid phases, ρ_g and ρ_l are the gas and liquid densities, g is the gravitational acceleration, and d is the pipe diameter.

According to Kataoka and Ishii (1987), pipes are classified as large-diameters when at their flow conditions d* is greater than 40, and small-diameter pipes are those which d* is smaller or equal to 18.5 (Shen, Hibiki, & Nakamura, 2015). For vertical two-phase flow in large-diameter pipes, Taylor bubbles, which are the main feature of Slug flow, are not stable. Therefore, slug flow does not exist at this condition. Some two-phase flow experimental studies in vertical pipes of large diameter (ID > 5 in) showed that only 1 out of 24 studies witnessed slug flow (Ali Shazia & Yeung, 2013), which can confirm the difference between large- and small-diameter pipes.

Figure 4a and 4b show the pipe diameters satisfying the concept of small and large diameter proposed by Kataoka and Ishii (1987) for Equation 2.1 for air-water and oil-gas flows, from atmospheric pressure to 3,000 psi. For oil-gas system, 30° API oil and gas with 96.5% methane are used for the calculations. It can be seen that, for air-water systems, the diameter which satisfies the large-diameter threshold of $d^* = 40$ slightly increases with pressure, while for oil-gas systems the diameter becomes smaller as pressure increases, being approximately 1 in at 3,000 psi and 60°F. This different trends of diameter size with pressure are mainly caused by differences of surface tension in the two systems, as the surface tension of crude oil and gas decreases significantly for higher pressures (Baker & Swerdloff, 1956), whereas for water it stays nearly constant.
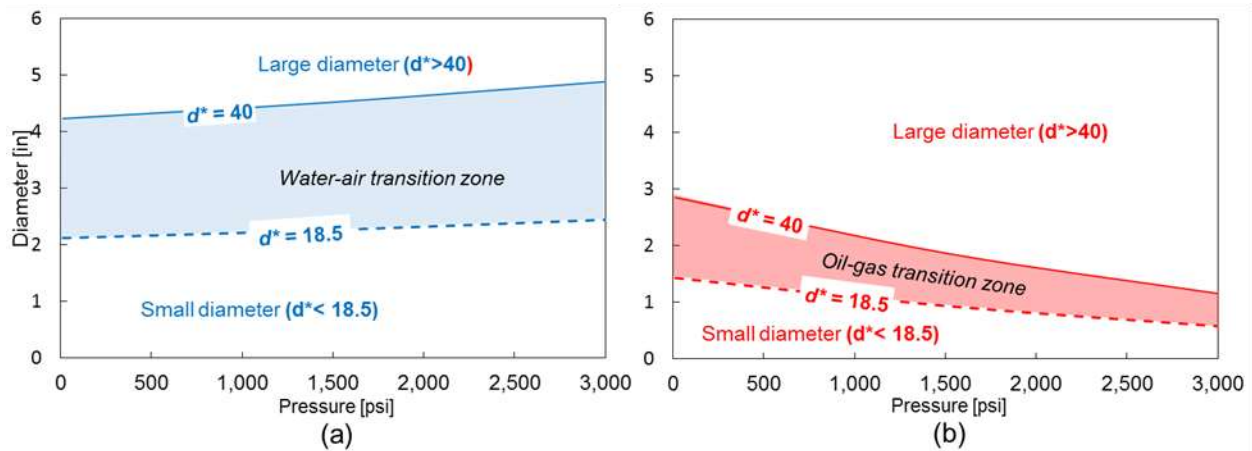
Figure 4 – Small and Large pipe diameter zones satisfying d*= 18.5 (dash lines) and d*= 40 (solid lines) for: a) air-water, and b) oil-gas systems. Diameters above the transition zones are considered large (e.g., absence of slug flow) and the diameters below the transition zones are considered small (e.g., the presence of slug flow is possible).

Most of the multiphase flow models are flow regime dependent, but as seen in Figure 4, *at high pressures Taylor bubbles (and consequently slug flow) might not be present on oil-gas flows for diameters as small as 1 inch*! The application of flow regime models for slug flow for pipe diameters between 1 and 4 inches is widely used in empirical and mechanistic models in the oil and gas industry. This may deliver erroneous results, as these wellbore flow models will try to predict possibly churn flow regime using a slug flow model. For this reason, it is crucial to implement the concept of small and large diameter in the models for a reliable prediction of pressure gradient in vertical two-phase flow in pipes.

2.4 TELES AND WALTRICH MODEL

A hybrid wellbore multiphase flow model has been developed at LSU to predict pressure gradient for all flow regimes in large-diameter pipes. This model consists of the combination of the mode proposed by Pagan, Williams, Kam, and Waltrich (2017), for churn and annular flow for large pipe diameters, with the empirical correlation of Duns and Ros (1963) for bubbly and slug flow. In addition, the hybrid model, herein referred as Teles and Waltrich model, also accounts for the concept of large and small diameter proposed by Kataoka and Ishii (1987). The purpose was to implement the concept of large and small diameter in order to identify whether slug flow occurs or not.

The main objective of Teles and Waltrich model is to accurately predict pressure gradient for oil and gas flow along large diameter pipes with high gas-liquid-ratios, as most of the models used to determine pressure drop along wells were originally developed and validated for air and water two-phase flow in pipe diameters smaller than 8 inches. A wide set of experimental and field data was used to evaluate the accuracy of this model, as well as for comparison with other commonly used empirical and mechanistic models.

2.4.1 PAGAN ET AL. (2017) MODEL

Pagan et al. (2017) proposed a steady-state model for calculating pressure gradient in churn and annular flow in large pipe diameters. The model is based on an approach proposed by Jayanti and Brauner (1994) for the churn flow regime in vertical pipes validated for small diameters. It consists on applying the concept of force balance in the gas core with length dl and cross-sectional area A_c, as shown in Figure 5. The gas core is represented by Figure 5a and the gas-liquid mixture is represented by Figure 5b.

(a)   (b)
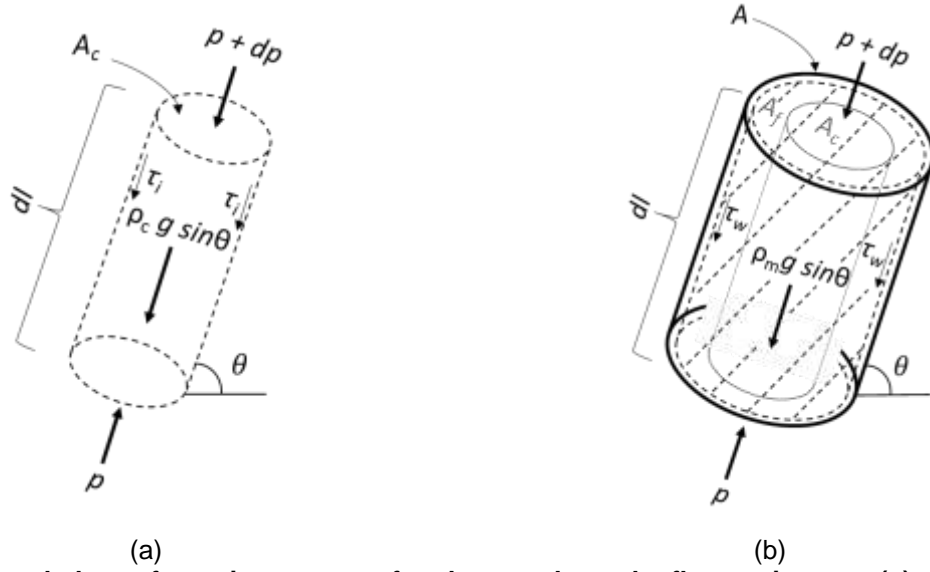
Figure 5 – Force balance for a pipe segment for churn and annular flow regimes on (a) gas core and (b) total cross-sectional area (including liquid film and gas core).

According to Pagan et al. (2017), both gas and liquid phases flow upward. In Figure 5a, the interaction between the gas and liquid phases is given by the shear stress (τ_i) at the gas-liquid interface. In addition, the force acting between the liquid phase and the pipe wall is represented by the wall shear tress (τ_w), as shown in Figure 5b. Neglecting the acceleration term, the momentum balance equation for both control volumes represented in Figure 5a and Figure 5b are given by the following expressions (Jayanti & Brauner, 1994),

$$-\frac{dp}{dl} = \frac{4\tau_i}{d\sqrt{\alpha}} + \rho_g g sin\theta \tag{2.2}$$

$$-\frac{dp}{dl} = \frac{4\tau_w}{d} + \left[\rho_g \alpha + \rho_l(1-\alpha)\right] g sin\theta \tag{2.3}$$

where dp/dl is the pressure gradient for the pipe segment dl, τ_i is the interfacial shear stress, τ_w is the wall shear stress, g is the gravitational acceleration, d is the diameter of the section, θ is the inclination angle with the horizontal, α is the void fraction, ρ_g and ρ_l are the gas and liquid densities. Equations 2.2 and 2.3 are solved for dp/dl and θ.

2.4.1.1 WALL AND INTERFACIAL SHEAR STRESS

In the churn flow regime, the liquid motion is oscillatory. However, the net liquid rate is upward. Thus, (Jayanti & Brauner, 1994) proposed that the average wall shear stress should be calculated based on the net liquid flow rate, neglecting the liquid flow variation with time. As in the annular flow regime, the net liquid film flows always upward along the pipe wall. The wall shear stress, τ_w, is calculated from the following relationship for both annular and churn flow regimes,

$$\tau_w = \frac{1}{2}\rho_l f_l \left(\frac{u_{sl}}{1-\alpha}\right)^2 \tag{2.4}$$

where u_{sl} is the superficial liquid velocity, and f_l is the friction factor of the liquid film. Equation 2.4 represents the wall shear stress for single-phase flow, considering that only the liquid phase is in contact with the pipe wall. For laminar flow in the liquid film, and Reynold number, Re_{lf} smaller than 2,100, the

Fanning friction factor given by Equation 2.5 is used. For turbulent flow, when Re_{lf} is greater than 2,100, Blasius Equation 2.6 for smooth pipes is used.

$$f_l = \frac{16}{Re_{lf}} \tag{2.5}$$

$$f_l = \frac{0.079}{Re_{lf}^{0.25}} \tag{2.6}$$

The Reynolds number if given by,

$$Re_{lf} = \frac{u_{lf}\rho_l d}{\mu_l} \tag{2.7}$$

where d is the pipe diameter, μ_l is the liquid viscosity, u_{lf} the actual liquid film velocity of the film, which is given by:

$$u_{lf} = \frac{u_{sl}}{1-\alpha} \tag{2.8}$$

The interfacial shear stress between the gas core and the liquid film shown in Figure 5a is calculated with the equation below:

$$\tau_i = \frac{1}{2}\rho_g f_i \left(\frac{u_{sg}}{\alpha}\right)^2 \tag{2.9}$$

where u_{sg} is the gas superficial velocity. Equation 2.9 can be used since the gas velocity is generally much larger than the liquid velocity when the fluids are flowing under churn or annular flow regimes. Thus, the liquid velocity is neglected, and the interfacial shear stress is calculated based on single-phase gas flow.

The study of Pagan et al. (2017) proposed that the interfacial friction factor should be calculated as suggested by Jayanti and Brauner (1994) by the average of $f_{i,W}$ and $f_{i,B}$ as shown below:

$$f_i = \frac{1}{2}\left(f_{i,W} + f_{i,B}\right) \tag{2.10}$$

However, instead of using the empirical correlation for $f_{i,W}$ proposed by Wallis (1969) assuming thin liquid films in pipes and $f_{i,B}$ correlation proposed by Bharathan, Richter, and Wallis (1978), it should be used the correlation of as suggested by (Alves, 2014), which leads to best results for churn and annular flow regimes, and it is given by:

$$f_{i,B} = 0.005 + 10^{\left(-0.56 + \frac{9.07}{d^*}\right)}\left[\frac{d^*(1-\alpha)}{4}\right]^{\left(1.63 + \frac{4.74}{d^*}\right)} \tag{2.11}$$

where d^* is the dimensionless diameter proposed by Kataoka and Ishii (1987) (equation 2.1). Pagan et al. (2017) proposes the use of the general equation for interfacial friction factor proposed by Wallis (1969) for $f_{i,W}$ as given by,

$$f_{i,W} = 0.005\left(1 + 300\frac{\delta}{D}\right) \tag{2.2}$$

where δ/D is the dimensionless liquid film thickness. The latter term can be represented in terms of void fraction (α), as the void fraction can be interpreted by the cross-sectional area of the gas core, A_c, divided

by the cross-sectional area of the pipe *A*. Thus, this study proposes Wallis (1969) modified interfacial friction factor without assumption of thin liquid film in pipes for churn flow regime, given by,

$$f_{i,W} = 0.005 + 0.75\,(1 - \sqrt{\alpha}) \tag{2.3}$$

Wallis (1969) modified interfacial friction factor equation with assumption of thin liquid film is used only for annular flow regime, given by,

$$f_{i,W} = 0.005 + 0.375\,(1 - \alpha) \tag{2.4}$$

2.4.2 DUNS AND ROS (1963)

Duns and Ros (1963) developed their model based in three different regions: bubbly, plug, and mist flow. This empirical model for pressure drop along the wellbore is a result of an intense laboratory study of 4,000 two phase flow tests. The experiments were carried out in vertical pipes with diameters ranging from 1.26 to 5.60 inches for gas-water flow (Brill & Mukherjee, 1999), and gas-diesel oil flows. In the hybrid model presented in this report, Duns and Ros correlation was chosen for bubbly and slug flow due to its good accuracy on predicting pressure drop in these flow regimes for air-water and gas-oil fluids, for a wide range of pipe diameters.

2.4.3 MODEL OVERVIEW

Figure 6 illustrates the graphical interface preliminary developed by Teles and Waltrich in order to run the simulations for pressure along wells. The algorithm developed is written on Visual Basic Application (VBA). The input data such as well characteristics, PVT properties, models, etc. can be easily inserted for the simulations run.

Figure 6 – Preliminary graphical interface for simulator for pressure along the well.

The flow chart shown in the Figure 7 illustrates how the algorithm of the proposed model works for the calculation of pressure in each section of the well. This algorithm is deployed for each length increment from a known pressure (for instance, from the wellhead) to the bottom of the well.

In the previous report from LSU to BOEM (Waltrich et al., 2017 - Award M15PC00007), the main conclusion of that experimental study was that any wellbore flow correlation tested would provide errors lower than 10% for slip ratios lower than the unit ($v_{sg}/v_{sl} < 1$). Thus, for slip ratios lower than the unit, the model of Duns and Ros (1963) is selected to calculate the pressure gradient in the wellbore for small diameters and any flow regime.
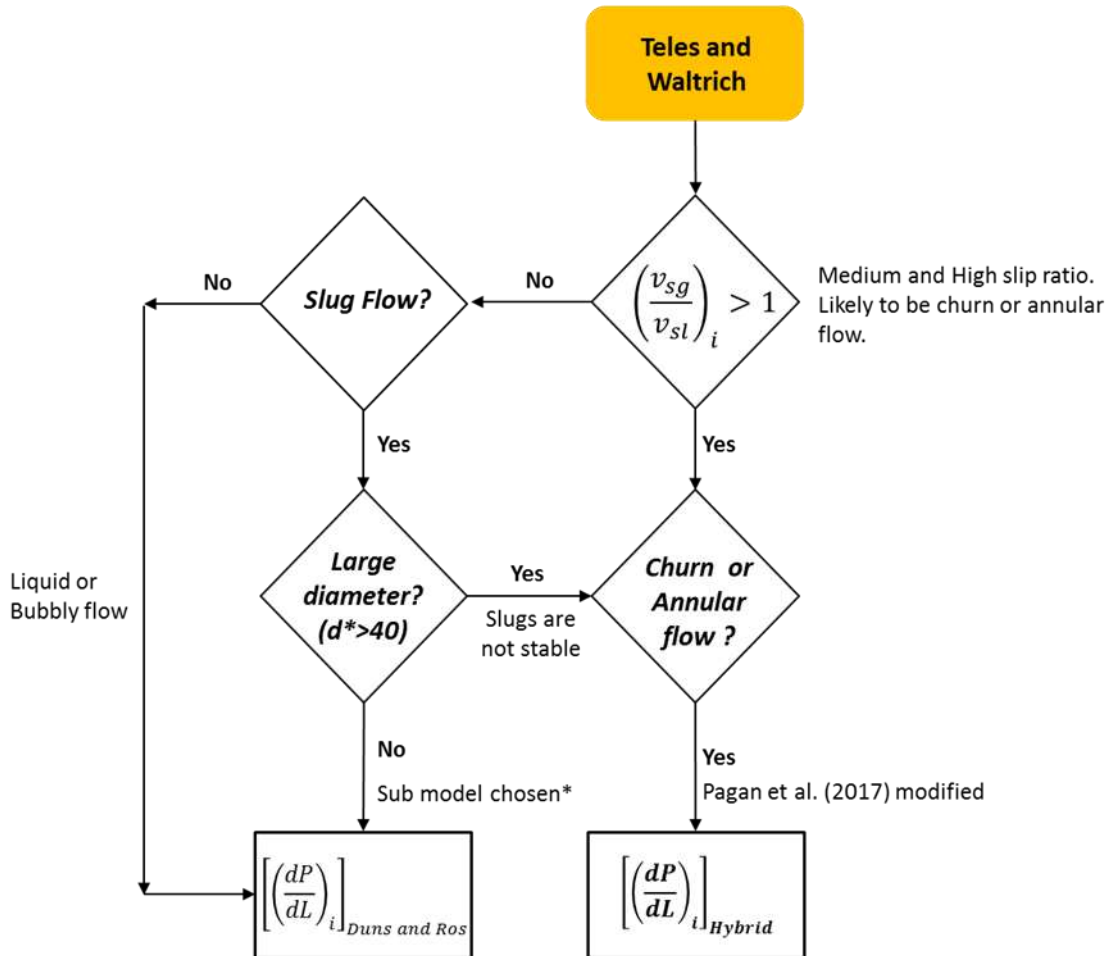
Figure 7 – Teles and Waltrich model workflow. The model uses Pagan et al. (2017) approach for churn and annular flow. *The chosen sub model for bubbly and slug flow in this study is Duns and Ros (1963).

3. RESULTS AND DISCUSSION

The accuracy of Teles and Waltrich model was compared to other models often found in commercial packages used for WCD calculations. These models are:

- Beggs and Brill (1973)
- Duns and Ros (1963)
- Mukherjee and Brill (1985)
- Hagedorn and Brown (1965)
- Gray (1974)
- Ansari, Sylvester, Cem, Ovadia, and Brill (1994)
- OLGA (2000)

The results from these models are compared to field data found in the literature (Asheim, 1986; Espanol, Holmes, & Brown, 1969; Fancher & Brown, 1963; Reinicke & Remer, 1987), and to the dataset of the experiments carried out at Louisiana State University's PERTT Lab for a previous research project funded by BOEM (Waltrich et al., 2017 - Award M15PC00007).

A summary of the experimental and field data used in this study to evaluate the models described is shown in Table 1.

Table 1 – Source and main characteristics of the database used to evaluate the performance of the Teles and Waltrich model and other commonly used correlations.

Source	Pipe ID [in]	Liquid flow rate [STB/d]	Gas-Liquid-Ratio [SCF/STB]	Fluids	Pressure [psi]
Fancher and Brown (1963)	2	75 – 936	525 – 7,283	Natural gas and oil	Up to 616
Reinicke et al. (1987)	3.98	7.5 – 493	7,734 – 1,403,645	Natural gas and water	Up to 8,880
Asheim (1986)	$\approx$ 4, 6.2	Up to 27,700	$\approx$ 325	Natural gas and oil	Up to 2,616
Espanol et al. (1969)	$\approx$ 2.4	1,656	Up to 9,975	Natural gas and oil	Up to 5,140
PERTT Lab	4, 8, 12	Up to 29,200	Up to 887	Air and water	$\approx$ 14.7
Petrobras	3.74, 4.5	Up to 1,100	Up to 2,600	Natural gas and oil	Up to 6,300
Statoil*	4.6	Up to 25,500	Up to 432	Natural gas and oil	Up to 5,200

*This set of data is in the process of being authorized by the company for usage in this study.

3.1 ERROR CALCULATION METHOD

The bottomhole pressure average absolute error for the results is calculated by:

$$Error\ (\%) = \frac{1}{n}\left(\sum_{i=1}^{n}|Error_{R,i}| \times 100\right) \tag{3.1}$$

where the relative error is:

$$Error_{R,i}\ (\%) = \frac{BHP|_{simulated} - BHP|_{measured}}{BHP|_{measured}} \tag{3.2}$$

and n is the number of experimental or field data points. The error bars included in Figures 9, 11, 13, 15, and 17 are represented by the standard deviation for the average absolute error for each scenario, which is calculated using the following expression,

$$Standard\ Deviation\ (\%) = \sum_{i=1}^{n} \sqrt{\frac{\left(Error - Error_{R,i}\right)^2}{n}} \tag{3.3}$$

The same procedure is applied for the LSU PERTT lab evaluation results, in this case the same the error is calculated based on pressure gradient instated of bottomhole pressure, given by,

$$Error_{R,i}\ (\%) = \frac{\left.\frac{dP}{dL}\right|_{simulated} - \left.\frac{dP}{dL}\right|_{measured}}{\left.\frac{dP}{dL}\right|_{measured}} \tag{3.4}$$

3.2 MODELS RESULTS FOR REINICKE ET AL. (1987) FIELD DATA

The data base of Reinicke and Remer (1987) consists of 26 gas-water wells for tubing diameter of 3.98 in, depth ranging from about 5,577 to 16,000 ft, slightly deviated wells (no more than 8 degrees from the vertical), liquid flowrates from 7.5 to 493 BBL/D, and gas-liquid ratios ranging from 7,734 to 1,403,645 SCF/STB.

Figure 8 shows the simulated and measured bottomhole pressures for all wells using the model of Teles and Waltrich and other flow models. The simulation results shows that the simulated bottomhole pressures for Teles and Waltrich model is within ± 20% deviation from the measured values. All other models presented errors higher than 20%, except the model of Hagedorn and Brown.

On Figure 9, the average absolute error and standard deviation of these errors for the simulation of the 24 wells of Reinicke and Remer (1987) using all flow models mentioned above are presented. These results show that for the Teles and Waltrich model, the error is within ± 14% in relation to the field data, while for the other models the error goes up to +45%, which is the case of Duns and Ros (1963). The error for the three mechanistic models are much higher when compared to Teles and Waltrich model. The predicted flow regime using Teles and Waltrich model was churn flow for most of the wells. On the other hand, Gray (1974), OLGA (2000), Ansari et al. (1994), Beggs and Brills, and Duns and Ros predicted that most of the wells flow in slug flow regime. According to the concept of large diameter defined by Katakoa and Ishii (1987), represented by Equation 2.1, it was observed that the dimensionless diameters (d^*) for all these wells are higher than 20 (ranging from 22 to 35), leading to the conclusion that at these conditions Taylor bubbles are not stable. Thus, slug flow should not occur. Therefore, the high errors in these models are likely due to the fact of they do not considering churn flow as a separated flow regime, and using slug flow model to determine the pressure gradient in churn flow regime. In these wells, the churn flow regime occurrence can be supported by the fact that the wells are deep, having large diameters and high pressures, conditions in which churn flow is most likely to occur, as shown in Figure 4. The fact that Hagedorn and Brown shows the second best performance for the evaluation of the field data may also corroborates the presence of churn flow. Hagedorn and Brown is not flow regime dependent and it also originally developed using experimental data for oil-gas systems. Thus, Hagedorn and Brown correlation should also incorporate the effects of surface tension showed in Figure 4, and may not include errors associated to using slug flow model as it is a flow regime independent correlation.
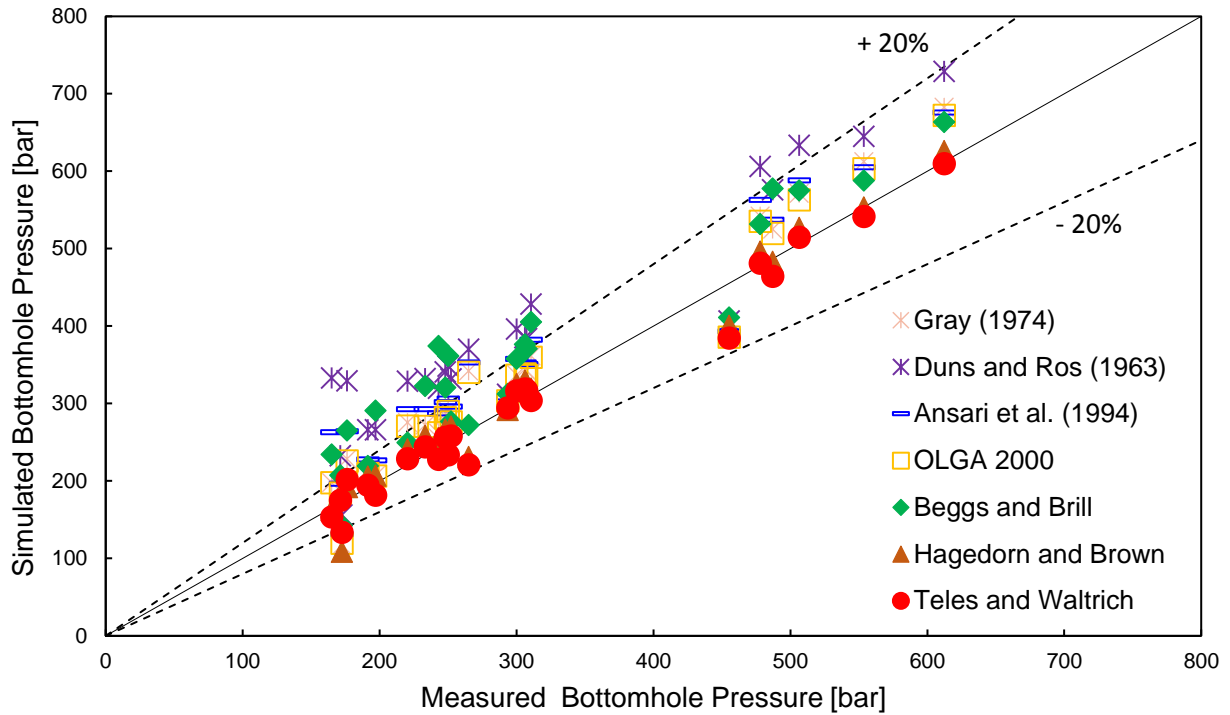
Figure 8 – Comparison of field bottomhole pressure and simulated bottomhole pressure for Teles and Waltrich; Gray (1974); Duns a Ros (1963); Ansari et al. (1994); OLGA (2000); Beggs and Brill; Hagedorn and Brown. The black dash lines represent the error line for ± 20% of the simulated pressure BHP.
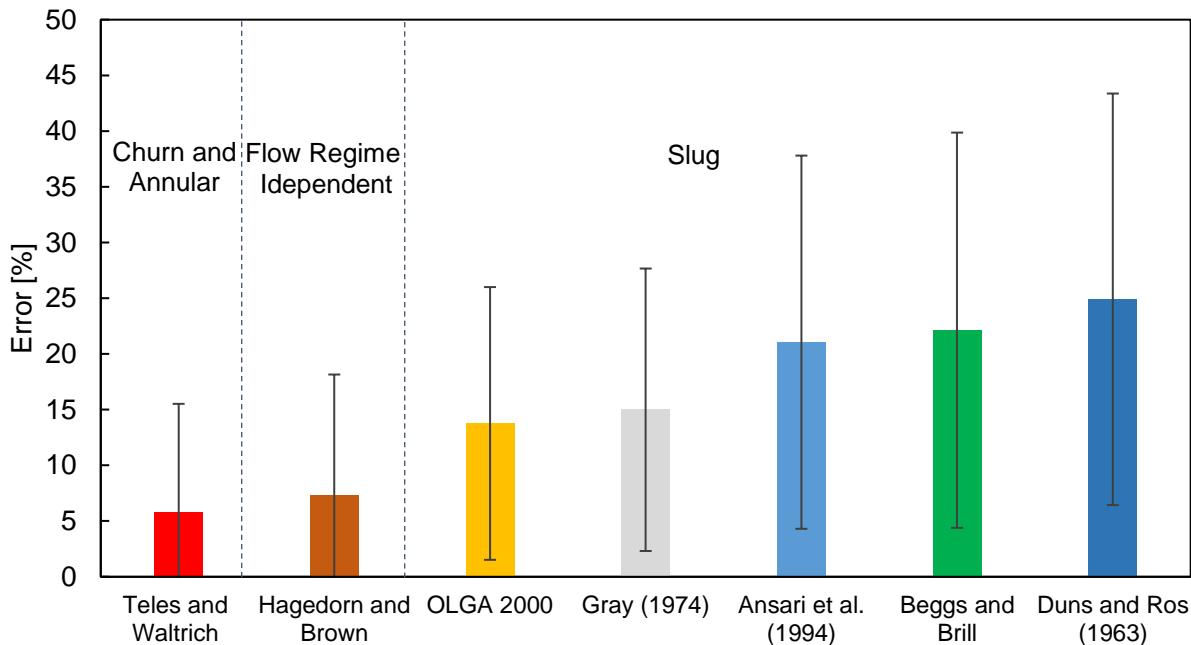
Figure 9 – Average absolute error and standard deviation of the errors for Teles and Waltrich, OLGA (2000), Gray (1974), Ansari et al. (1994), Beggs and Brill, Hagedorn and Brown, Duns and Ros (1963). The columns represent the average absolute error and the line intervals the standard deviations.

17

3.3 EVALUATION OF TWO-PHASE FLOW MODELS FOR LOUISIANA STATE UNIVERSITY'S PERTT LAB EXPERIMENTS

An experimental campaign was carried out at Louisiana State University's PERTT Lab to cover large diameter pipes and high liquid and gas velocity flows. The data from this data set includes 130 tests conducted for diameters 3.82, 7.80, and 11.7 in. The fluids used were air and water, the liquid superficial velocities range from 0.30 ft/s up to 14.3 ft/s, and air superficial velocities from 0.23 ft/s up to 103.6 ft/s. In some of the tests, the flow regimes were observed with a high speed camera. The data collected from those experiments were reported by Waltrich et al. (2017) and will be used in this work to evaluate the accuracy of the Teles and Waltrich model. Figure 10(a) to 10(g) present the vertical lift performance curves generated by this model for each liquid superficial velocity.

Teles and Waltrich model shows a reasonable match for low superficial velocities which are the cases from Figure 10(a) and 10(b) for all diameters, and Figure 10(c) for 4 and 12 in. For higher liquid velocities the model under predicted the pressure gradient for high gas velocities, while for low liquid superficial velocities the model overestimated the pressure gradient. It was observed that for large pipe diameters, the model in this study also showed a performance similar to the Hagedorn and Brown model for all tests, with errors from around 30% and up to 50%.

Figure 11(a) to 11(e) shown the results of the errors of pressure gradient for different levels of gas-liquid superficial velocity (slip) ratios for Teles and Waltrich, Duns and Ros, Beggs and Briil, Mukherjee and Brill, and Hagedorn and Brown models. It can be observed that for low slip ratio (v_{sg}/v_{sl}<1) all models have lower errors, therefore a good agreement with the experimental data. For medium slip ratio (1< v_{sg}/v_{sl} <100) the errors are higher for all models, except for Hagedorn and Brown. The high slip ratios (v_{sg}/v_{sl} >100) are the ones with the highest errors, going up to more than 100% for Teles and Waltrich model. Figure 12 illustrates the average absolute error of pressure gradient for the 4, 8, and 12 in pipes for Teles and Waltrich, Duns and Ros, Beggs and Briil, Mukherjee and Brill, and Hagedorn and Brown. In addition, Figure 13 shows the overall average absolute error of pressure gradient for all models mentioned.
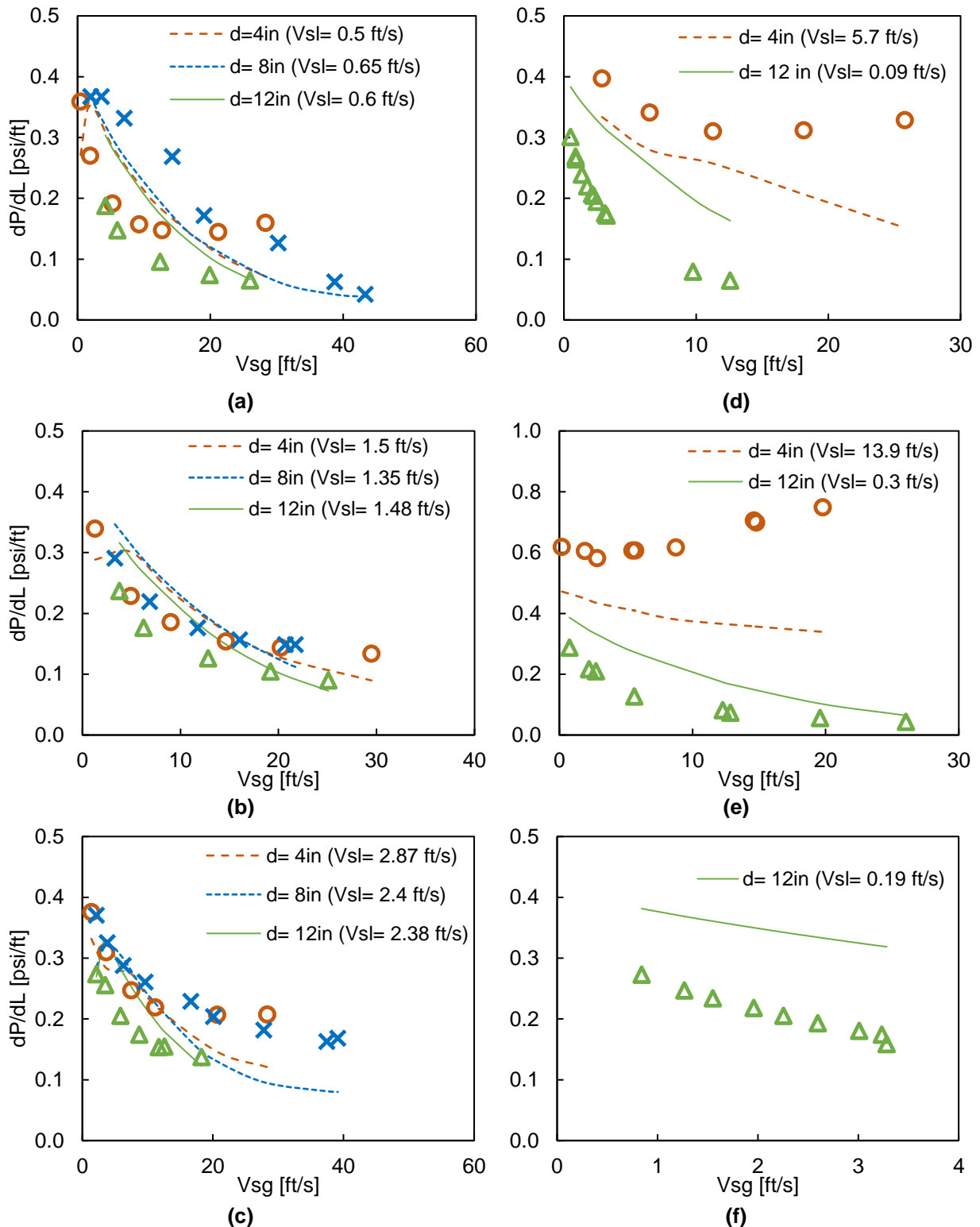
Figure 10 – Comparison between Teles and Waltrich model and experimental results in terms of pressure gradient versus gas superficial velocities for 4, 8, and 12 in pipe diameter and superficial liquid velocities from 0.09 to 13.9 ft/s (Figures 10a to 10f).
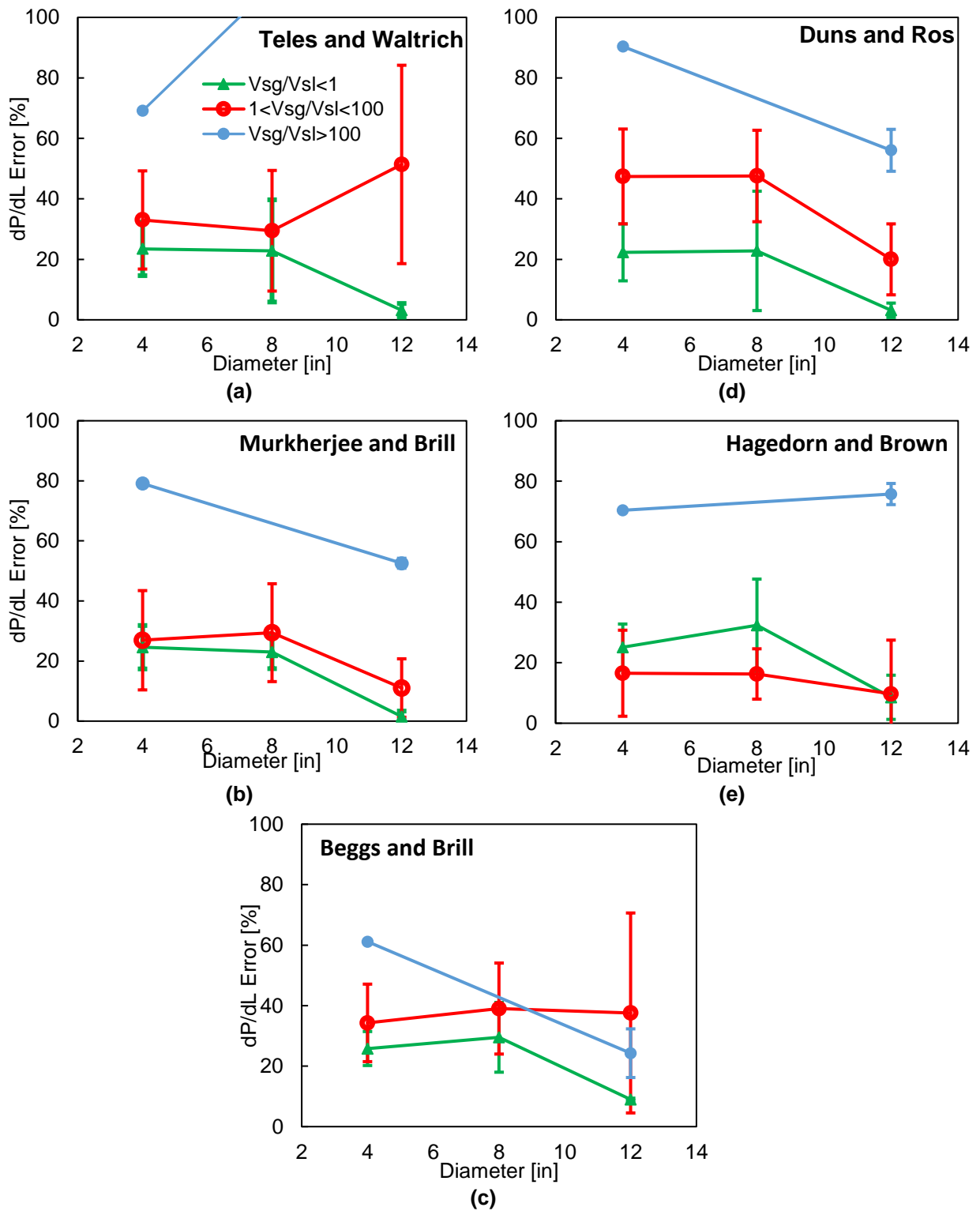
Figure 11 – Comparison errors of pressure gradient in terms of slip velocity for 4, 8, and 12 in pipe diameter for Teles and Waltrich, Duns and Ros, Beggs and Brill, Murkherjee and Brill, and Hagedorn and Brown models. Green curves represents scenarios having: slip ratio less than one; red curves: slip ratio between one and 100; blue curves: slip ratio greater than 100.
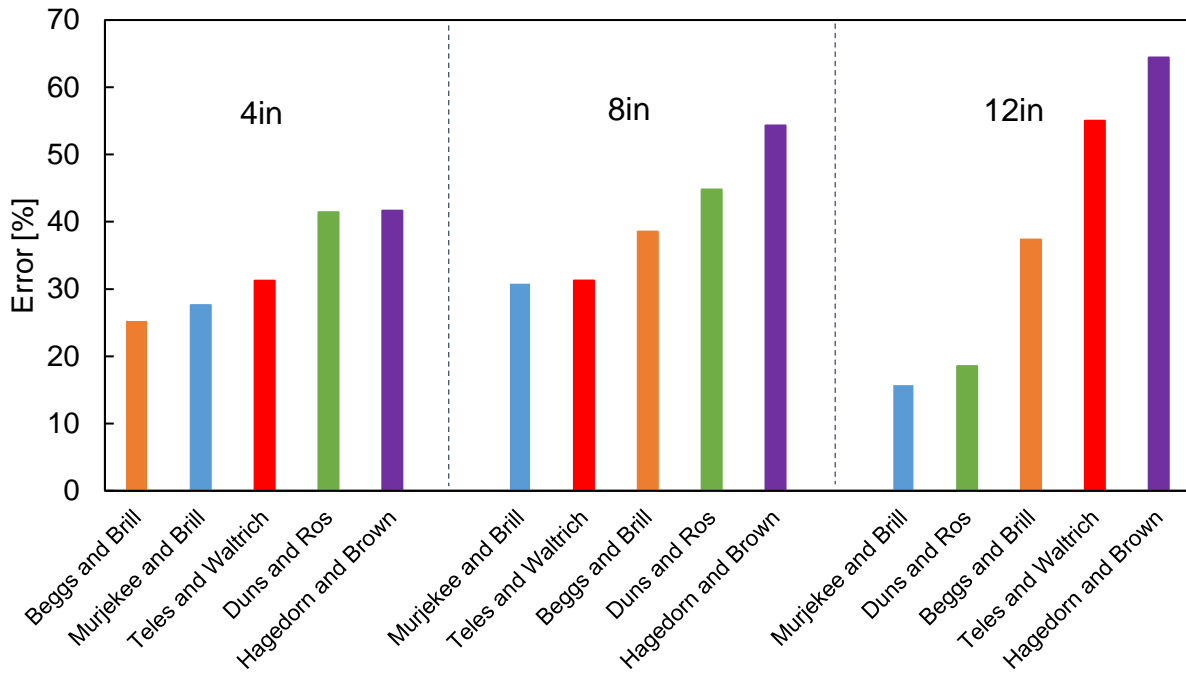
Figure 12 – Average Absolute Error of pressure gradient in % for Teles and Waltrich, Duns and Ros, Beggs and Brill, Murkherjee and Brill, and Hagedorn and Brown models for 4, 8, and 12in for the LSU/PERTT Lab experimental data reported by Waltrich et al. (2017).
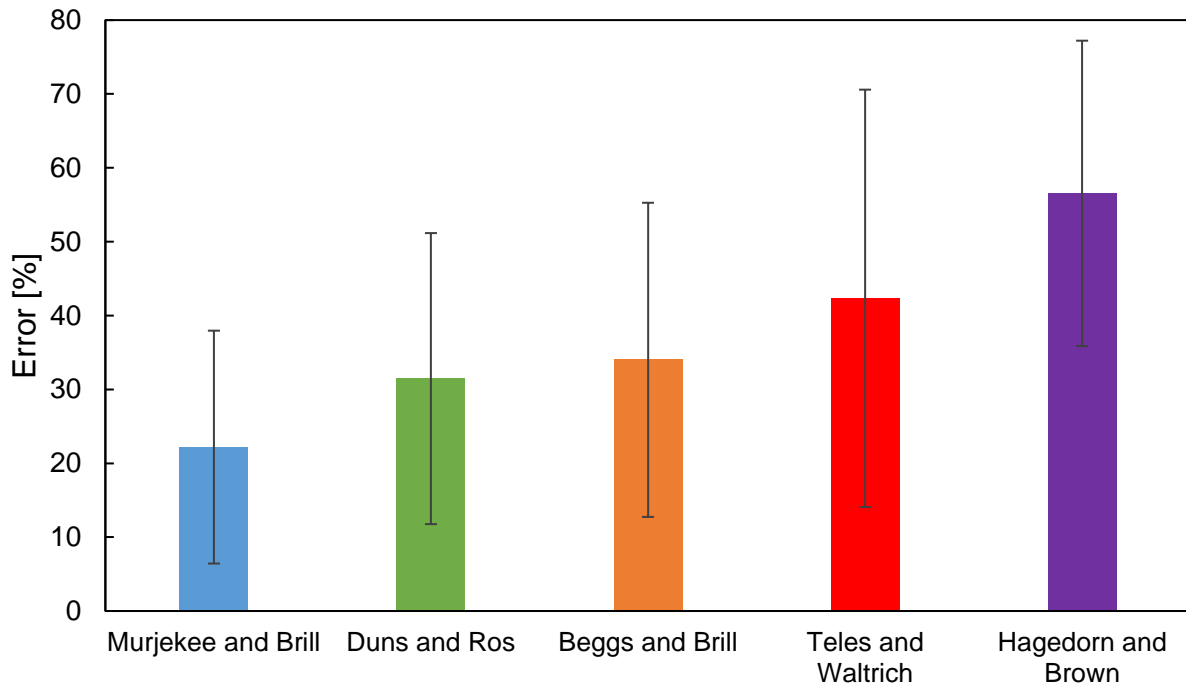
Figure 13 – Overall average absolute error of pressure gradient in % for Teles and Waltrich, Duns and Ros, Beggs and Brill, Murkherjee and Brill, and Hagedorn and Brown models for for the LSU/PERTT Lab experimental data reported by Waltrich et al. (2017).

Interestingly, as shown in Figure 12, all models evaluated for this database showed lower error for the 12 in pipe. For this pipe diameter, the error of Teles and Waltrich model is the second largest one, being over 50%. Looking at overall average error on Figure 13, the hybrid model shows a relatively high error when predicting pressure gradient. Further investigation should be done for this experimental set of data. It was expected the proposed model to have the best results, since it is differently from the other models, Teles and Waltrich is for large diameter and high flow rates. It is important to mention that the flow regime prediction from Teles and Waltrich model agreed with the flow regime recorded by the high speed camera being most of them churn and annular flow.

3.4 EVALUATION OF TWO-PHASE FLOW MODELS FOR FANCHER AND BROWN (1986) FIELD DATA

Fancher and Brown (1986) conducted tests in an 8,000 ft vertical well with 2 in ID. The tested liquid flow rates range from 75 to 936 BBL/D, and gas-liquid ratios from 525 to 7,283 SCF/BBL. The gas rates were set by the continuous injection of a gas with specific gravity of 0.57 through a gas lift valve located at 2,774 ft in the well. The produced oil has 34 API gravity of at 60 °F, and the produced rates were controlled by a downhole choke. A linear profile of fluid temperature was assumed from the bottomhole to the wellhead. The pressure profile along 12 wells were predicted using the Pagan et al. (2017), Beggs and Brill, Hagedorn and brown models, and the proposed hybrid model of Teles and Waltrich. Figure 14(a) to 14(m) show the comparison between the results obtained with these models and the field data.

Teles and Waltrich model showed a reasonable fit to the field data of Fancher and Brown (1986). From the graphs below, it can be observed that for high GLR this model has a better fit than the other models, since at high flowrates of gas flow regime is more likely to be either churn or annular. It was also observed that for a liquid rate of 144 BBL/D, when the GLR increases Beggs and Brill and Hagedorn and brown deviate from the field data trend. This is probably due to the fact that Beggs and Brill do not consider churn flow and Hagedorn and brown is independent of flow regime, what lead to higher errors when predicting the pressure gradient in either churn or annular flow conditions.
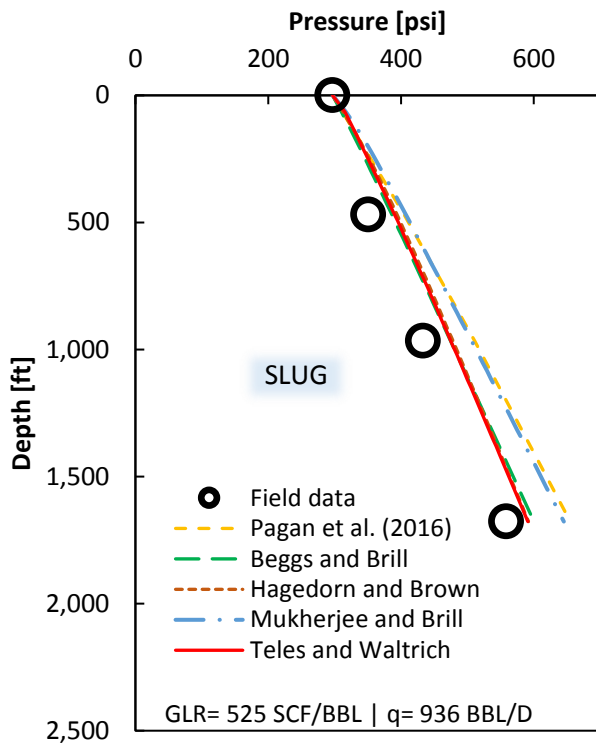
(a)
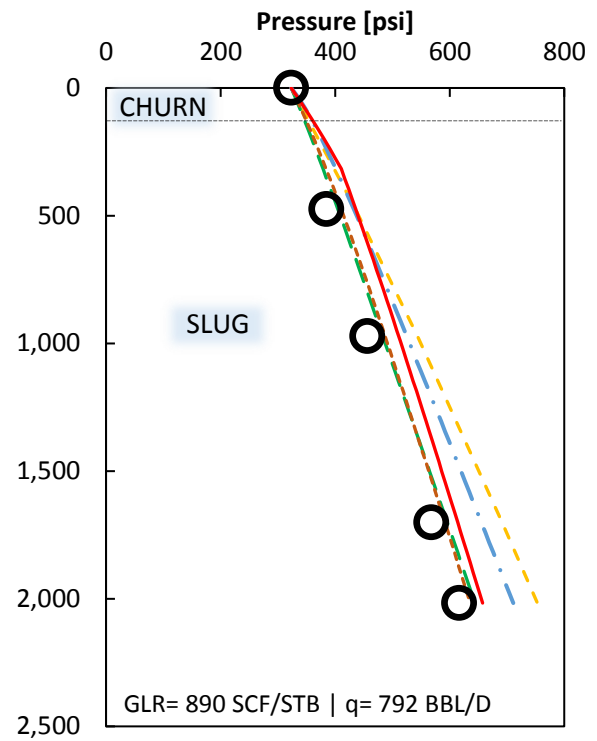
(b)
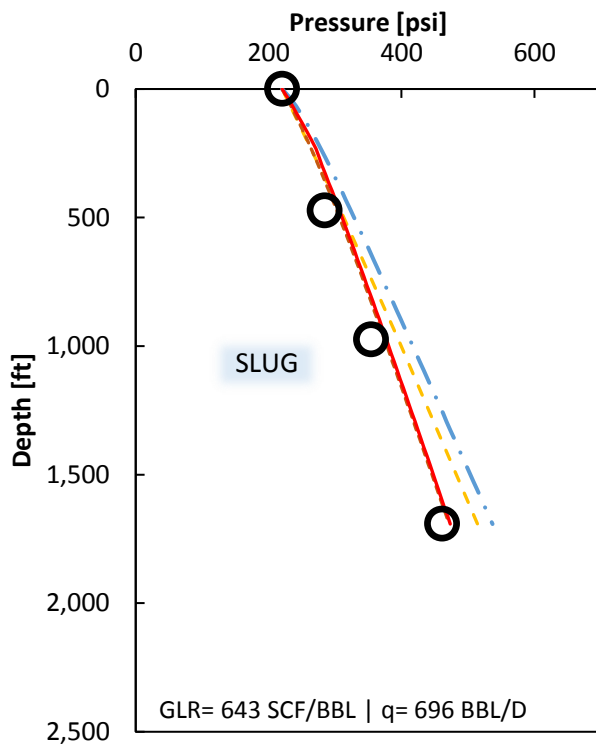
(c)
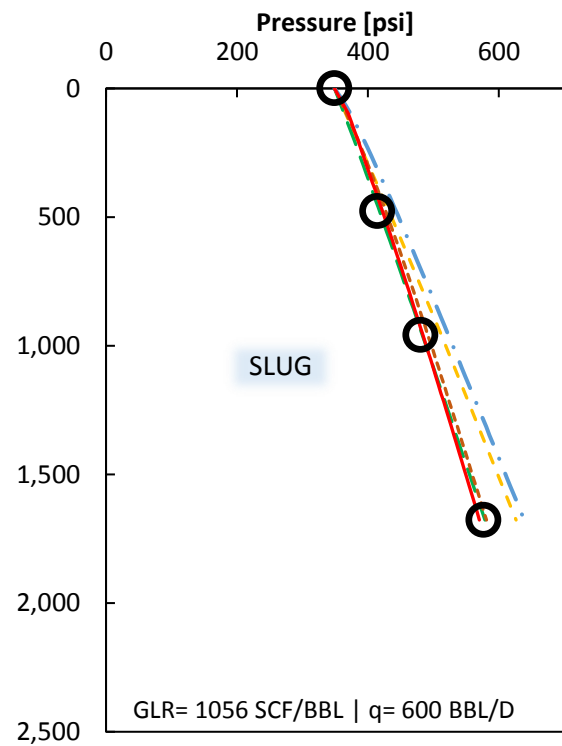
(d)
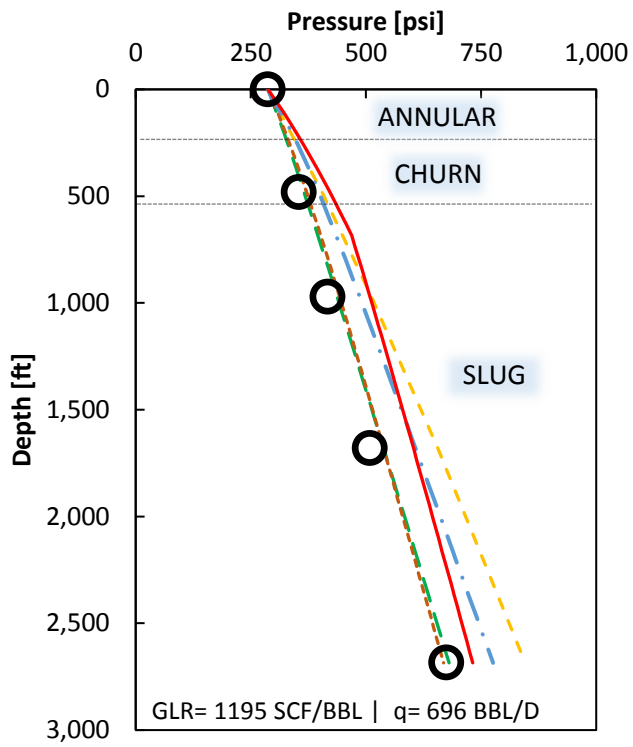
(e)
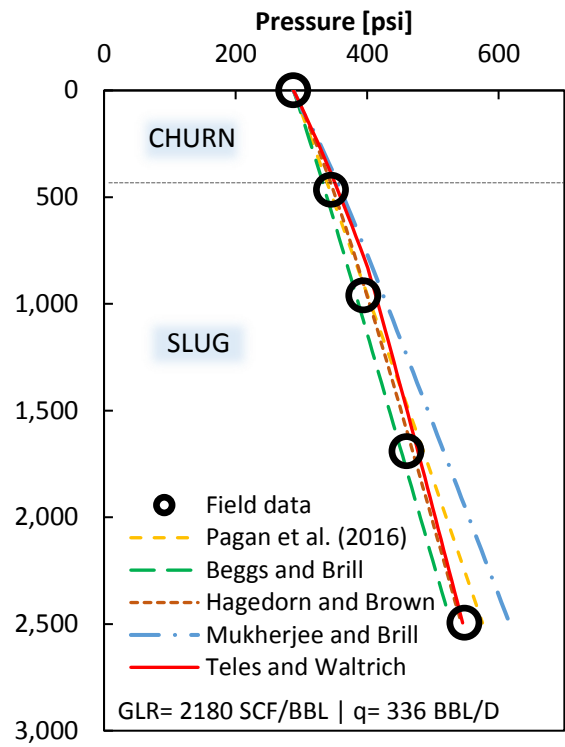
(f)
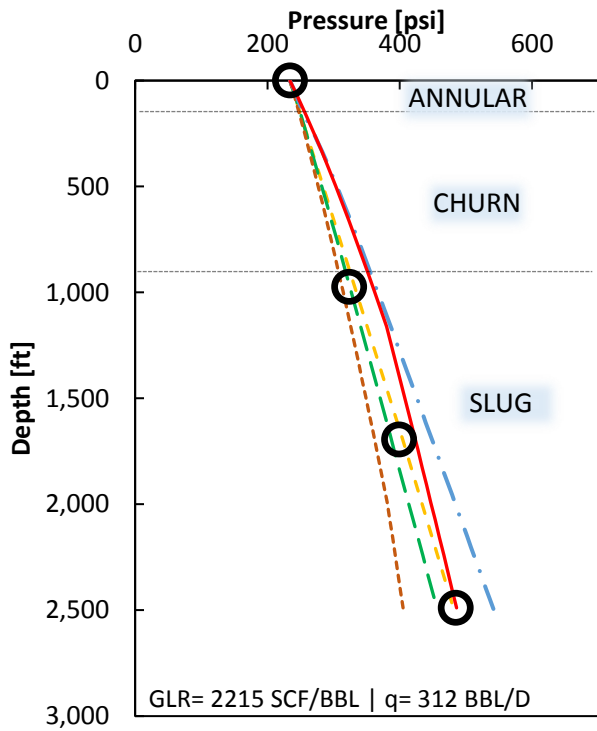
(g)
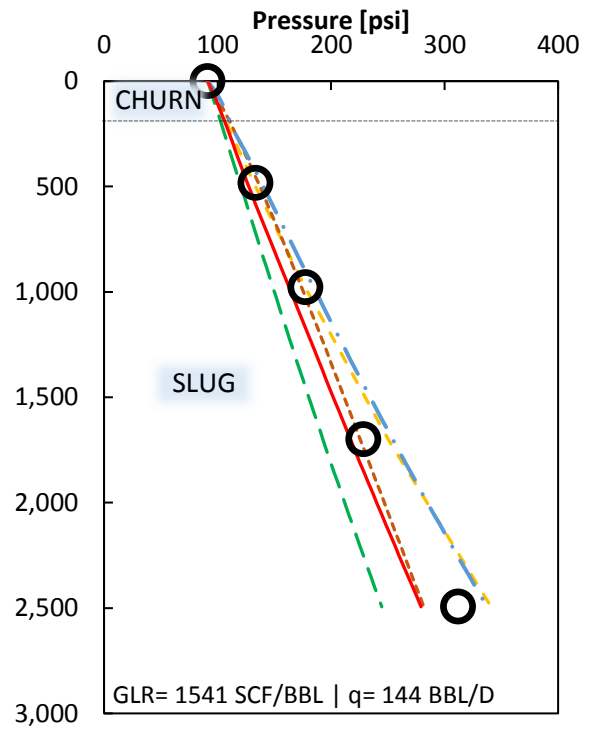
(h)
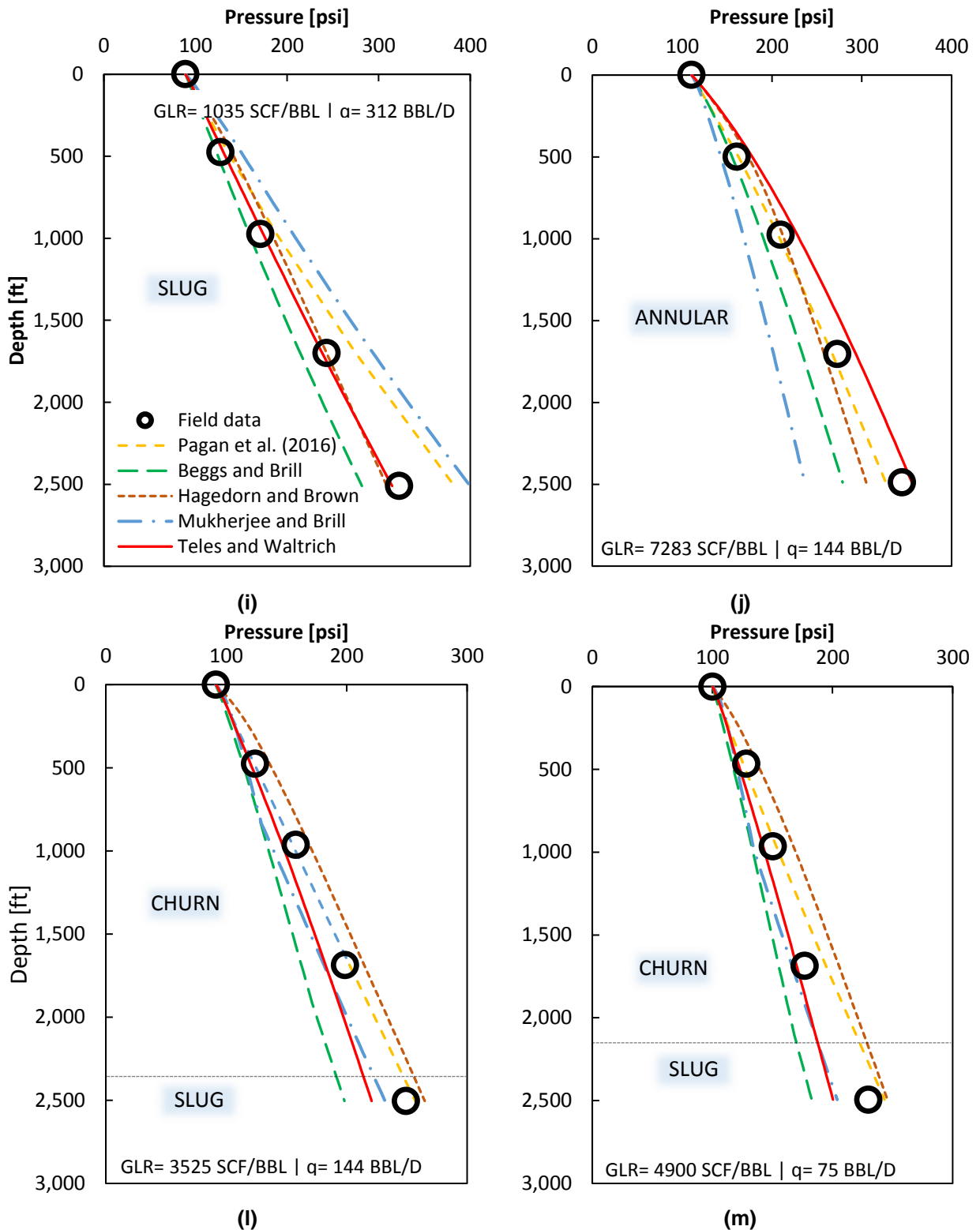
Figure 14 – Comparison between simulation results using the model proposed in this study and measured wellbore pressure profile (field data from Fancher and Brown, 1963). Circles represent the measured pressures and continuous lines are the simulated pressures. The horizontal dash lines represent the transition of flow regime along the well.
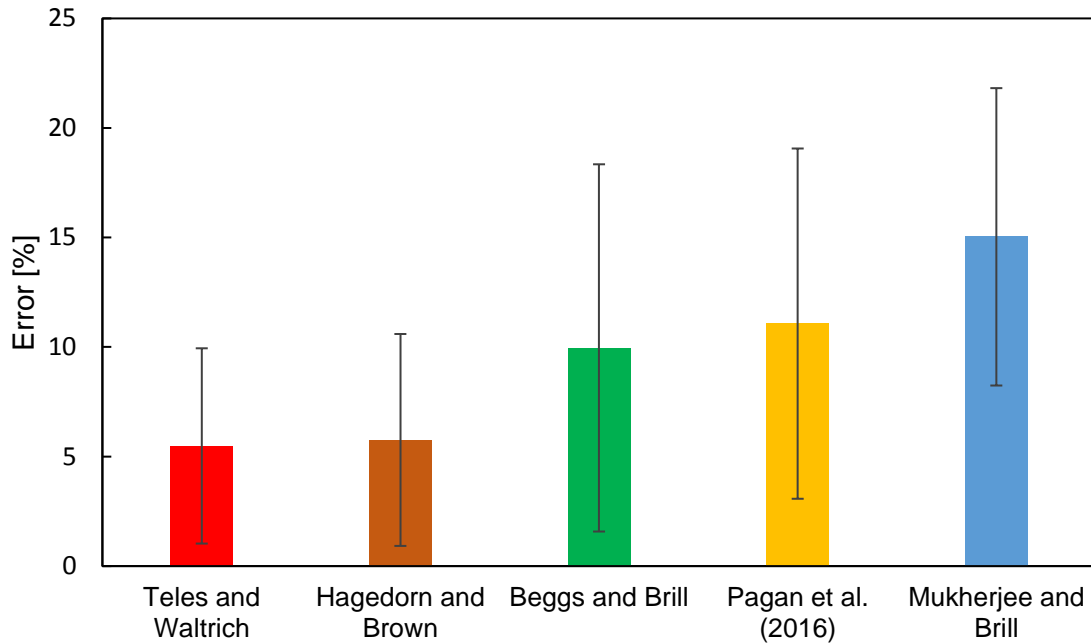
Figure 15 – Average absolute error of the simulated bottomhole pressure for Teles and Waltrich, Hagedorn and Brown, Mukherjee and Brill, Beggs and Brill, and Pagan et al. (2016), for Fancher and Brown (1963) field data. The standard deviation of the errors are represented by the error bars on each model.

A comparison of the average absolute error of simulated bottomhole pressure for the 12 wells is given on Figure 15. It was observed that Teles and Waltrich model had an average absolute error very similar to Hagedorn and Brown model, up to 11% (standard deviation bar) in wells with low GLR. On the other hand, for high gas-liquid ratio scenarios, where churn flow and annular flow were predicted, the errors for Teles and Waltrich model were lower than 1%. This model had the lowest average absolute error for the 12 wells. Differently from the experimental data analysis of air-water systems from the previous section, for this field data, Mukherjee and Brill model had the highest error.

3.5 EVALUATION OF TELES AND WALTRICH MODEL FOR DEVIATED WELLS FROM ASHEIM (1986) FIELD DATA

The field data from the Forties Field were used to evaluate the accuracy of the proposed hybrid model for deviated wells. The set of data from Asheim (1986) consists of 37 runs in an oil and gas well, with oil rates from 6,540 to 27,270 STB/D and GOR of 337 SFC/STB for the 6.184 in ID and 323 SCF/STB for the 3.958 in ID wells. For all runs, the oil and gas specific gravity are 0.84 and 1.1, respectively. The depth of the point of pressure measurement varies from 6,900 ft to 10,300 ft. Figure 16 shows the comparison of measured and simulated bottomhole pressure for the 37 scenarios. It should be noted that the error of the simulated BHP is within ± 20%.

The purpose of this analysis is to also evaluate pressure drop for large diameter piper for more field data. This system includes field data with wellbore flowing oil and natural gas, moderate high flow rates. The simulated data showed good agreement with the field data, and the error in the prediction using the simulator is consistent.
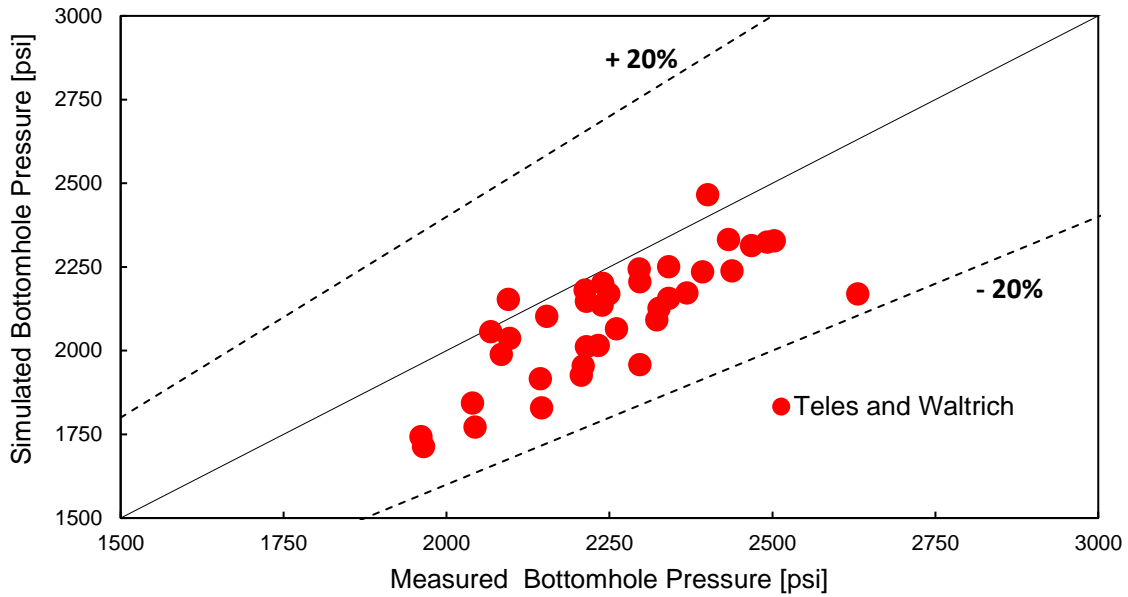
Figure 16 – Comparison of field bottomhole pressure and simulated bottomhole pressure for Teles and Waltrich for 34 well in Forties field from Asheim (1986). The black dash lines represent the error line for ± 20% of the simulated pressure BHP.

Besides Teles and Waltrich model, this set of data for inclined well from Asheim (1986) was also simulated for other models: Mukherjee and Brill, Duns and Ros, Beggs and Brill, and Hagedorn and Brown. Figure 17 shows the comparison of the average absolute error for all these models. Teles and Waltrich model has a good agreement with the field data, having an average absolute error of about 6.5 % (represented by the red box). This model had similar results from Beggs and Brill, which already is a widely used model for deviated wells.
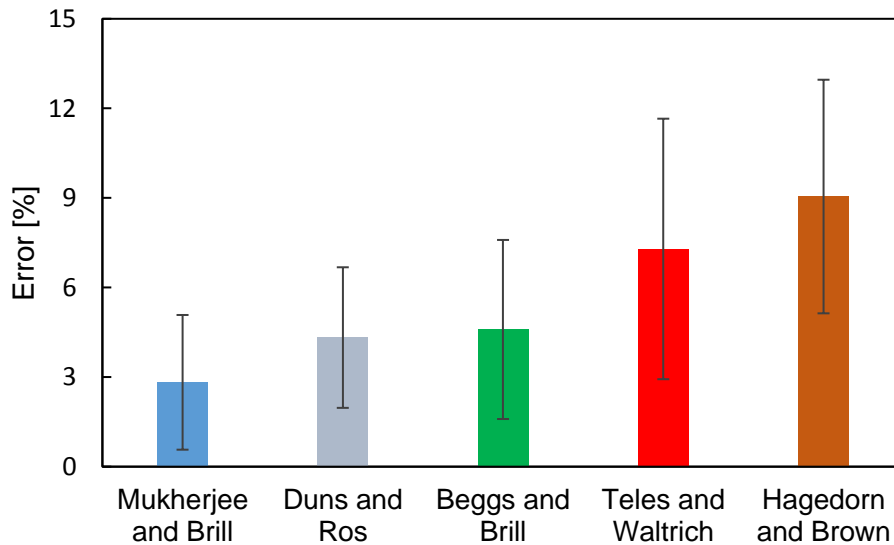
Figure 17 – Average absolute error of the simulated bottomhole pressure for Teles and Waltrich, Mukherjee and Brill, Hagedorn and Brown, Beggs and Brill, and Duns and Ros for Asheim (1986) field data. The standard deviation of the errors are represented by the error bars on each model.

3.6 EVALUATION OF TELES AND WALTRICH MODEL USING FIELD DATA FROM ESPANOL ET AL. (1969)

This database consists of 44 tests performed in a 2.376 in ID well flowing with oil rates up to 1,656 BBL/D and gas-oil ratios from 171 to 9,975 SCF/BBL. These data were reported by Espanol et al. (1989) and Aziz and Govier (1972). For these oil wells the API gravity ranges from 18 to 44 and depth goes up to 12,450 ft. Figure 18 shows preliminary results for the evaluation of Teles and Waltrich model for 10 out of the 48 wells. It was observed that the simulated values of bottomhole pressures are close to the measured values, with the highest error of 14.3%. For these field data, further investigation and comparison of empirical and mechanistic models should be carried out in the next weeks.
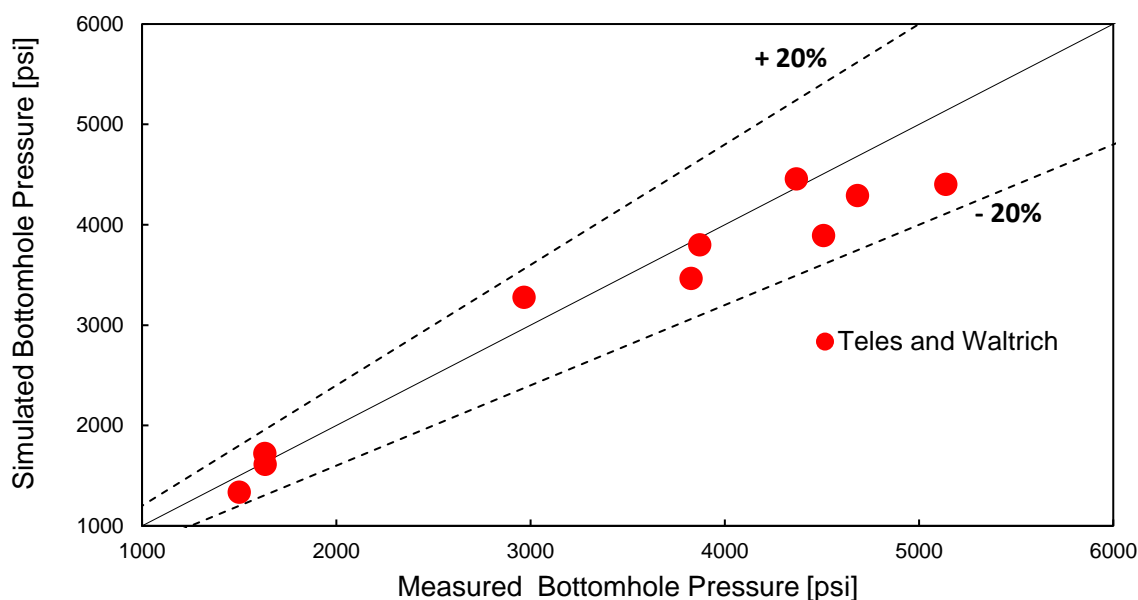
Figure 18 – Comparison of field bottomhole pressure and simulated bottomhole pressure for Teles and Waltrich for Espanol et al. (1989) data set. The black dash lines represent the error line for ± 20% of the simulated pressure BHP.

3.7 PETROBRAS AMERICA

This data consists of two condensate gas wells in the Gulf of Mexico. These wells have diameters of 3.74 and 4.5 in. The Gas Liquid Ratio are up to 2,600 SCF/STB with pressure up to 6,300 psi. The evaluation of the models for this data set will be performed in the next four weeks.

3.8 STATOIL

This data consists of an oil well with 4.6 in ID, with high liquid rate, up to 25,500 STB/D and Gas Liquid Ratio of 432 SCF/STB. The pressure is around 5,200 psi. The evaluation of the models for this data set will be likely performed after Statoil authorizes dataset to be used in this study.

4. CONCLUSIONS

- For the field data of high gas-liquid-ratio flows, Teles and Waltrich model showed a better performance than the other empirical and mechanistic models such as OLGA (2000), Gray, Beggs and Brill, Murjekee and Brill, Duns and Ros, and Hagedorn and Brown. Average absolute error for Teles and Waltrich was about 5% while for the other flow regime dependent models it was up to 25%.

- With Reinicke and Remer (1987) data set evaluation, it was concluded that considering slug flow when there is churn flow leads to significant errors. Therefore, churn flow needs to be modeled separately in order to obtain accurate results. Hagedorn and Brown, as a flow regime independent model, has low errors. However, this model was not accurate when evaluating the other field and experimental data.

- Teles and Waltrich model has a reasonable accuracy for two-phase flow in inclined wells. This model only underestimates the bottomhole pressure by at most 17% for a 20 degrees deviated well.

- For the experimental results from PERTT Lab, Teles and Waltrich model did not show an accuracy as good as Murjekee and Brill, Beggs and Brill, Duns and Ros. The average absolute error of pressure gradient was around 42%. As the other models Teles and Waltrich also showed higher errors for pressured gradient prediction in scenarios with slip ratio greater than one unit. This can also be observed in the pressure gradient versus gas superficial velocity plots when simulated pressure starts deviating from measured pressure for higher gas superficial velocities. The results of the analysis of experimental data (air-water) from PERTT Lab were not as expected for Teles and Waltrich model. It was observed that this model had an excellent accuracy for field data (oil-natural gas and water-natural gas), what leads us to investigate more the set of data and simulations performed for the experimental case.

- More investigation should be done in order to properly validate the model. The final report will contain evaluation of more field data (i.e. Petrobras America and Statoil), as well as the analysis of the hybrid model combined with correlations that have showed good accuracy in this study, such as Mukherjee and Brill.

REFERENCES

Ali, S. F. (2009). *Two phase flow in large diameter vertical riser.* (PhD), Cranfield University, School of Engineering, Department of Process and System Engineering,

Ali Shazia, F., & Yeung, H. (2013). Two-phase flow patterns in large diameter vertical pipes. *Asia-Pacific Journal of Chemical Engineering, 9*(1), 105-116. doi:10.1002/apj.1750

Alves, M. V. C. (2014). *Modelagem Numerica do Escoamento Transient Churn-Annular em Tubulacoes Verticais e sua Aplicacao na Simulacao de Carga de Liquido em Pocos de Gas.* Universidade Federal de Santa Catarina, Florianopolis, Santa Catarina

Ansari, A. M., Sylvester, N. D., Cem, S., Ovadia, S., & Brill, J. P. (1994). Supplement to SPE 20630, A Comprehensive Mechanistic Model for Upward Two-Phase Flow in Wellbores. In: Society of Petroleum Engineers.

Asheim, H. (1986). MONA, An Accurate Two-Phase Well Flow Model Based on Phase Slippage. doi:10.2118/12989-PA

Aziz, K., & Govier, G. W. (1972). Pressure Drop In Wells Producing Oil And Gas. doi:10.2118/72-03-04

Baker, O., & Swerdloff, W. (1956). Calculation of Surface Tension 6 - Finding Surface Tension of Hydrocarbon Liquids. *Oil and Gas Journal*, 125.

Beggs, D. H., & Brill, J. P. (1973). A Study of Two-Phase Flow in Inclined Pipes. doi:10.2118/4007-PA

Bharathan, D., Richter, H. J., & Wallis, G. B. (1978). *Air-water counter-current annular flow in vertical tubes. Report EPBI-NP-786*. Retrieved from

Brill, J. P., & Mukherjee, H. K. (1999). *Multiphase Flow in Wells*: Henry L. Doherty Memorial Fund of AIME, Society of Petroleum Engineers.

Buchholz, K., Krieger, A., Rowe, J., Etkin, D. S., McCay, D. F., Gearon, M. S., . . . Turner, J. (2016). *Oil Spill Response Plan (OSRP) Equipment Capabilities Review - Task 1: Worst Case Discharge Analysis*. Retrieved from

Capovilla, M. S., Cavalcanti de Sousa, P., & Waltrich, P. J. (2017). *Experimental investigation of vertical high-velocity two-phase flows in large-diameter pipes*. Paper presented at the 18th International Conference on Multiphase Production Technology, Cannes, France.

Cheng, H., Hills, J. H., & Azzorpardi, B. J. (1998). A study of the bubble-to-slug transition in vertical gas-liquid flow in columns of different diameter. *International Journal of Multiphase Flow, 24*(3), 431-452. doi:https://doi.org/10.1016/S0301-9322(97)00067-0

Duns, H., Jr., & Ros, N. C. J. (1963). *Vertical flow of gas and liquid mixtures in wells*. Paper presented at the 6th World Petroleum Congress, Frankfurt am Main, Germany.

Economides, M. J., Hill, A. D., Ehlig-Economides, C., & Zhu, D. (2012). *Petroleum Production Systems*: Pearson Education.

Espanol, J. H., Holmes, C. S., & Brown, K. E. (1969). *A Comparison of Existing Multiphase Flow Methods for the Calculation of Pressure Drop in Vertical Wells*. Paper presented at the Fall Meeting of the Society of Petroleum Engineers of AIME, Denver, Colorado.

Fancher, G. H., Jr., & Brown, K. E. (1963). Prediction of Pressure Gradients for Multiphase Flow in Tubing. doi:10.2118/440-PA

Gray, H. E. (1974). *Vertical Flow Correlation in Gas Wells. User's Manual for API 148 Subsurface Controlled Safety Valve Sizing Computer Program, Appendix B*. Retrieved from

Guet, S., & Ooms, G. (2005). FLUID MECHANICAL ASPECTS OF THE GAS-LIFT TECHNIQUE. *Annual Review of Fluid Mechanics, 38*(1), 225-249. doi:10.1146/annurev.fluid.38.061505.093942

Hagedorn, A. R., & Brown, K. E. (1965). Experimental Study of Pressure Gradients Occurring During Continuous Two-Phase Flow in Small-Diameter Vertical Conduits. doi:10.2118/940-PA

Hernandez-Perez, V., Zangana, M., Kaji, R., & Azzopardi, B. J. (2010). *Effect of pipe diameter on pressure drop in vertical twophase flow*. Paper presented at the 7th International Conference on Multiphase Flow ICMF Tampa, FL USA.

Hibiki, T., & Ishii, M. (2000). Experimental study on hot-leg U-bend two-phase natural circulation in a loop with a large diameter pipe. *Nuclear Engineering and Design, 195*(1), 69-84. doi:https://doi.org/10.1016/S0029-5493(99)00176-4

Jayanti, S., & Brauner, N. (1994). CHURN FLOW. *8*(1-4), 471-521. doi:10.1615/MultScienTechn.v8.i1-4.90

Kataoka, I., & Ishii, M. (1987). Drift flux model for large diameter pipe and new correlation for pool void fraction. *International Journal of Heat and Mass Transfer, 30*(9), 1927-1939. doi:https://doi.org/10.1016/0017-9310(87)90251-1

Mukherjee, H., & Brill, J. P. (1985). Pressure Drop Correlations for Inclined Two-Phase Flow. *Journal of Energy Resources Technology, 107*(4), 549-554. doi:10.1115/1.3231233

Ohnuki, A., & Akimoto, H. (1996). An experimental study on developing air-water two-phase flow along a large vertical pipe: effect of air injection method. *International Journal of Multiphase Flow, 22*(6), 1143-1154. doi:https://doi.org/10.1016/0301-9322(96)00039-0

Ohnuki, A., & Akimoto, H. (2000). *Experimental Study on Transition of Flow Pattern and Phase Distribution in Upward Air–Water Two-Phase Flow Along a Large Vertical Pipe* (Vol. 26).

OLGA. (2000). Dynamic Multiphase Flow Simulator: Schlumberger.

Omebere-Iyari, N. K., Azzopardi, B. J., & Ladam, Y. (2007). Two-phase flow patterns in large diameter vertical pipes at high pressures. *AIChE Journal, 53*(10), 2493-2504. doi:10.1002/aic.11288

Pagan, E., Williams, W. C., Kam, S., & Waltrich, P. J. (2017). A simplified model for churn and annular flow regimes in small- and large-diameter pipes. *Chemical Engineering Science, 162*, 309-321. doi:https://doi.org/10.1016/j.ces.2016.12.059

Reinicke, K. M., & Remer, R. J. (1987). Comparison of Measured and Predicted Pressure Drops in Tubing for High-Water-Cut Gas Wells. doi:10.2118/13279-PA

Schlegel, J. P., Sawant, P., Paranjape, S., Ozar, B., Hibiki, T., & Ishii, M. (2009). Void fraction and flow regime in adiabatic upward two-phase flow in large diameter vertical pipes. *Nuclear Engineering and Design, 239*(12), 2864-2874. doi:https://doi.org/10.1016/j.nucengdes.2009.08.004

Schoppa, W., Zabaras, G. J., Menon, R., & Wicks, M. (2013). *Gaps and Advancements for Deepwater Production and Remote Processing: Large Diameter Riser Laboratory Gas-Lift Tests*. Paper presented at the Offshore Technology Conference, Houston, Texas, USA.

Shen, X., Hibiki, T., & Nakamura, H. (2015). Bubbly-to-cap bubbly flow transition in a long-26m vertical large diameter pipe at low liquid flow rate. *International Journal of Heat and Fluid Flow, 52*, 140-155. doi:https://doi.org/10.1016/j.ijheatfluidflow.2015.01.001

Shoham, O. (2006). *Mechanistic Modeling of Gas-Liquid Two-Phase Flow in Pipes*.

Shoukri, M., Hassan, I., & Gerges, I. (2008). Two-Phase Bubbly Flow Structure in Large-Diameter Vertical Pipes. *The Canadian Journal of Chemical Engineering, 81*(2), 205-211. doi:10.1002/cjce.5450810205

Smith, T. R., Schlegel, J. P., Hibiki, T., & Ishii, M. (2012). Two-phase flow structure in large diameter pipes. *International Journal of Heat and Fluid Flow, 33*(1), 156-167. doi:https://doi.org/10.1016/j.ijheatfluidflow.2011.10.008

SPE. (2015). Calculation of Worst-Case Discharge (WCD). In: Society of Petroleum Engineers.

Takacs, G. (2001). *Considerations on the Selection of an Optimum Vertical Multiphase Pressure Drop Prediction Model for Oil Wells*. Paper presented at the SPE/ICoTA Coiled Tubing Roundtable, Houston, Texas.

Wallis, G. B. (1969). One-dimensional two-phase flow.

Waltrich, P. J., Capovilla, M. S., Lee, W., Zulqarnain, M., Hughes, R., Tyagi, M., . . . Griffith, C. (2017). *Experimental Evaluation of Wellbore Flow Models Applied to Worst-Case-Discharge Calculations*. Paper presented at the SPE Health, Safety, Security, Environment, & Social Responsibility Conference - North America, New Orleans, Louisiana, USA.

Wu, B., Firouzi, M., Mitchell, T., Rufford, T. E., Leonardi, C., & Towler, B. (2017). A critical review of flow maps for gas-liquid flows in vertical pipes and annuli. *Chemical Engineering Journal, 326*, 350-377. doi:https://doi.org/10.1016/j.cej.2017.05.135

Zulqarnain, M. (2015). *Deepwater Gulf of Mexico oil spill scenarios development and their associated risk assessment.* (PhD), Louisiana State University, Baton Rouge, LA.